International Journal of Theoretical Physics (2024) 63:260
https://doi.org/10.1007/s10773-024-05800-x

RESEARCH

# Simulating Nonlinear Radiation Diffusion Through Quantum Computing

**Frank Gaitan[1] · Frank Graziani[2] · Max D. Porter[3]**

Received: 1 August 2024 / Accepted: 4 October 2024


**Abstract**
The recent success of the fusion ignition experiment at Lawrence-Livermore National Laboratory has renewed excitement for inertial confinement fusion. Designing such experiments relies on computational modeling using radiation hydrodynamic codes run on massively parallel supercomputers which simulate hydrodynamic flows, radiation diffusion, and thermonuclear burn. Constructing a quantum algorithm for radiation hydrodynamics that provides a quantum speedup is of great interest. A recent quantum algorithm that solves the Navier-Stokes equations of hydrodynamics with a quadratic speedup marks a first step towards this goal. Here we take the next step and present a quantum algorithm for nonlinear radiation diffusion that also has a quadratic speedup. To verify the algorithm we consider radiation striking a cold, optically thick target that generates a Marshak wave in the target. Results of numerical simulation of the quantum algorithm are compared with those of a standard partial differential equation solver and excellent agreement is found.

**Keywords** Quantum algorithms · Nonlinear radiation diffusion · Quantum simulation

## 1 Introduction

The never ending need for clean, plentiful energy has been an important driver for science and technology development in nuclear fusion. The recent achievement of ignition during an inertial confinement fusion (ICF) experiment at Lawrence-Livermore National Laboratory [1–4] is a significant milestone that has generated great excitement. The plan and design of such an ICF experiment relies heavily on computational modeling based on radiation hydrodynamic codes such as Hydra [5, 6] and Flash [7–9] that run on massively parallel supercomputers, and which simulate hydrodynamic flows, radiation diffusion, and thermonuclear burn. Such simulations are computationally expensive, with 3D simulations requiring millions of hours of CPU time, and as much as 30 days to complete.

Given the difficulty of radiation hydrodynamics simulations, it is natural to ask whether a quantum computer might speed up these simulations. A first step towards constructing a

✉ Frank Gaitan
fgaitan@lps.umd.edu

[1] Laboratory for Physical Sciences, 8050 Greenmead Dr, College Park 20740, MD, USA

[2] Lawrence-Livermore National Laboratory, 7000 East Avenue, Livermore 94550, CA, USA

[3] Sandia National Laboratory, 1515 Eubank SE, Albuquerque 87123, NM, USA

Published online: 11 October 2024

quantum algorithm for radiation hydrodynamics is already possible as a quantum algorithm for simulating hydrodynamic flows exists that provides a quadratic speedup [10]. This quantum algorithm, which solves the nonlinear Navier-Stokes equations, was soon extended to a quantum algorithm for solving systems of nonlinear partial differential equations (PDE) [11] with a quadratic speedup. Here we take a second step towards a quantum radiation hydrodynamics algorithm by showing how the quantum PDE (QPDE) algorithm [11] can be used to simulate the nonlinear dynamics of radiation diffusion with a quadratic speedup.

The structure of this Paper is as follows. We first briefly describe the physical assumptions leading to radiation diffusion and write down the nonlinear PDE that governs its time development (Section 2). We then explain how the QPDE algorithm can be used to solve the nonlinear radiation diffusion equation (Section 3). To verify the quantum algorithm we apply it to the problem of radiation striking a cold, optically thick target that causes a Marshak wave [12] to propagate through the target. We numerically simulate application of the QPDE algorithm to this problem and compare the results found with those obtained using a standard PDE solver (Section 4). The agreement is excellent. Finally, we close with some directions for future work (Section 5).

## 2 Nonlinear Radiation Diffusion

At the heart of every ICF experiment are tens of thousands of multi-physics simulations using radiation hydrodynamic (RH) multi-physics codes that provide design support, and improve the experiment's chances for success. In RH simulations, the modeling of radiation transport presents an exciting, but challenging obstacle. Indeed, in RH multi-physics codes, radiation transport tends to dominate CPU time. The radiative transfer equation is semi-classical in nature. In the kinetic equation, the photons are treated like any other gas. The quantum mechanical effects enter through the absorption, emission and scattering terms. Each of these three processes describes, at a micro-physical level, the quantum mechanical interaction of matter and radiation. The challenges of solving the radiation transport problem has led researchers to solve a simpler problem. In many applications where the plasma is dense (such as in ICF) the diffusion approximation to the full transport problem is an excellent approximation. By going to the diffusion limit of the transport equation, the number of degrees of freedom in 3D are reduced from seven to five for multi-group and seven to four for Planckian. This approximation is by far the most used approximation in RH multi-physics codes. Underlying the Planckian radiation diffusion equation is the concept of local thermodynamic equilibrium [13, 14] which supposes collisions in the plasma are sufficiently frequent that local thermodynamic equilibrium is quickly established with local temperature $T(\mathbf{x}, t)$. Furthermore, the plasma is assumed to be optically thick so that the photon mean free path is small compared to the length scale over which local (thermal) equilibrium varies, causing the radiation to come into local equilibrium with the plasma. The optical thickness also causes the radiation specific intensity to be weakly anisotropic, and the radiation energy flux to be proportional to the spatial gradient of the radiation energy density $\varepsilon(\mathbf{x}, t)$. Under these conditions, the radiation transport equation reduces to the nonlinear radiation diffusion equation (NRDE):

$$\frac{\partial \varepsilon}{\partial t} - \nabla \cdot \left[ \frac{c}{3} \lambda_R(\rho, T) \nabla \varepsilon \right] = 0. \tag{1}$$

Here $\varepsilon = aT^4; a = 8\pi^5 k^4 / 15 h^3 c^3; \lambda_R(\rho, T)$ is the Rosseland mean free path (see below); and $\rho(\mathbf{x}, t)$ is the fluid mass density. The solution satisfies the initial condition $\varepsilon(\mathbf{x}, 0) =$

$\varepsilon_0(\mathbf{x})$, and in the verification problem below, Dirichlet boundary conditions $\varepsilon(\mathbf{y}, t) = g(\mathbf{y}, t)$, where $\mathbf{y}$ is a point on the boundary.

## 3 Quantum PDE Algorithm

We now describe how the QPDE algorithm [10, 11] is applied to the NRDE. The result is a quantum radiation diffusion (QRD) algorithm, which at its coarsest level of description consists of two steps.

The first step is to discretize space while leaving time as a continuous parameter. Thus the spatial continuum parameterized by $\mathbf{x}$ is replaced by a spatial grid containing $M$ uniformly spaced grid-points parameterized by $\mathbf{x}(\mathbf{I}) = \mathbf{x}_0 + \mathbf{I}\Delta$, where $\mathbf{I} = (i_1, i_2, i_3)$, $1 \leq i_k \leq m_k$ $(k = 1, 2, 3)$, $M = m_1 m_2 m_3$, and $\Delta$ is the spacing between grid-points along any coordinate direction. The radiation energy density $\varepsilon(\mathbf{x}, t)$ is now restricted to grid-points: $\varepsilon_{\mathbf{I}}(t) \equiv \varepsilon(\mathbf{x}(\mathbf{I}), t)$. Absent a spatial continuum, spatial partial derivatives no longer exist and must be approximated. There are many ways to do this. Here we use a finite difference approximation. This replaces spatial partial derivatives of $\varepsilon(\mathbf{x}, t)$ with algebraic expressions of the $\{\varepsilon_{\mathbf{I}}(t)\}$. As will be discussed below, approximation of the spatial divergence term in the NRDE leads to an algebraic expression $f_{\mathbf{I}}(\varepsilon)$ at each grid-point $\mathbf{x}(\mathbf{I})$. Time $t$ is now the only continuous parameter and so the partial time derivative in the NRDE becomes a total derivative. The result of the spatial discretization is the reduction of the NRDE to a coupled set of ordinary differential equations (ODEs),

$$\frac{d\varepsilon_{\mathbf{I}}}{dt} = f_{\mathbf{I}}(\varepsilon), \tag{2}$$

with an ODE associated with each grid-point $\mathbf{x}(\mathbf{I})$. We will determine the driver functions $\{f_{\mathbf{I}}(\varepsilon)\}$ below. The initial and boundary conditions for (2) are obtained by evaluating the initial and boundary conditions of the NRDE at the grid-points $\mathbf{x}(\mathbf{I})$.

The second step is to use a quantum nonlinear ODE algorithm to solve (2). Refs. [10, 11] used a quantum algorithm due to Kacewicz [15], though any quantum nonlinear ODE algorithm would do. We briefly describe the application of Kacewicz' algorithm to (2). To unclutter the notation, we will suppress the subscripts on $\varepsilon_{\mathbf{I}}(t)$ and $f_{\mathbf{I}}(t)$. Kacewicz' algorithm returns an approximate, bound solution $\alpha(t)$ to the exact solution $\varepsilon(t)$ of (2) over the time interval $0 \leq t \leq T$. The algorithm: guarantees the error in the approximate solution is less than $\epsilon$ with probability $1 - \delta$, where $\epsilon$ and $\delta$ are user-supplied; and gives a quadratic speedup over classical nonlinear ODE algorithms [15].

Kacewicz' algorithm consists of five steps. The first partitions the time interval $0 \leq t \leq T$ into $n$ primary subintervals by introducing $n + 1$ uniformly spaced intermediate times $t_0 = 0, \ldots, t_i = ih, \ldots, t_n = T$, where $h = T/n$. The $i^{th}$ primary subinterval $[t_i, t_{i+1}]$ is denoted $T_i$, with $i = 0, \ldots, n-1$. Step-two partitions each primary subinterval $T_i$ into $N_k = n^{k-1}$ secondary subintervals by introducing $N_k + 1$ uniformly spaced intermediate times $t_{i,0} = t_i, \ldots, t_{i,j} = t_i + j\bar{h}, \ldots, t_{N_k} = t_{i+1}$, where $\bar{h} = h/N_k = T/n^k$. The $j^{th}$ secondary subinterval $[t_{i,j}, t_{i,j+1}]$ in $T_i$ is denoted $T_{i,j}$. The third step associates with each primary subinterval $T_i$ a parameter $y_i$. The parameter $y_0$ is set equal to the ODE initial condition, $y_0 \equiv \varepsilon_0$, while the remaining parameters $y_1, \ldots, y_{n-1}$ approximate the exact solution $\varepsilon(t)$ at the times $t_1, \ldots, t_{n-1}$, respectively. (Step-five will explain how these $n - 1$ parameters are assigned values.) Step-four uses Taylor's method [16, 17] to approximate the exact solution

$\varepsilon(t)$ in each of the secondary subintervals $T_{i,j}$ using a truncated Taylor series $\alpha_{i,j}(t)$ expanded about the time $t_{i,j}$. The approximate solution $\alpha_i(t)$ in primary subinterval $T_i$ is defined by $\alpha_i(t) = \alpha_{i,j}(t)$ for $t \in T_{i,j}$, and is required to be continuous throughout $T_i$. Thus $\alpha_{i,j}(t)$ and $\alpha_{i,j+1}(t)$ must agree at their common boundary time $t_{i,j+1}$: $\alpha_{i,j}(t_{i,j+1}) = \alpha_{i,j+1}(t_{i,j+1})$. The final condition placed on $\alpha_i(t)$ is that $\alpha_i(t_i) \equiv y_i$. The fifth step derives a relation that allows the $\{y_i\}$ to be determined iteratively:

$$y_{i+1} = y_i + \int_{t_i}^{t_{i+1}} dt\ f(\alpha_i(t)) \qquad (0 \le i \le n-2). \tag{3}$$

Kacewicz' algorithm uses a quantum integration algorithm to evaluate the integral on the RHS of (3). It is important to appreciate that this is the only task in this quantum algorithm that requires a quantum computer. All other calculations are done on a classical computer. In the work reported below, we use Novak's quantum integration algorithm [18] to evaluate the integrals. The procedure for determining the $\{y_i\}$ begins with $y_0 \equiv \varepsilon_0$. Knowing $y_0$ determines the approximate solution $\alpha_0(t)$ (see Refs. [10, 11, 15] for details). Inserting $\alpha_0(t)$ into the ODE driver function $f(\varepsilon)$ determines the integrand in (3) for $i = 0$. Novak's quantum algorithm is used to approximate the integral and the value returned is (classically) added to $y_0$ to give $y_1$. Knowing $y_1$ gives $\alpha_1(t)$ which is substituted into $f(\varepsilon)$ and its integral over $T_1$ is approximated using Novak's algorithm. The value returned is added to $y_1$ to give $y_2$, etc. At the end of the iteration procedure all approximate solutions $\alpha_0(t), \ldots, \alpha_{n-1}(t)$ are determined and the approximate ODE solution is $\alpha(t) = \alpha_i(t)$ for $t \in T_i$.

Kacewicz [15] showed that his quantum nonlinear ODE algorithm provides a quadratic quantum speedup over classical nonlinear ODE algorithms. Refs. [10] and [11] then showed that the QPDE algorithm inherits this quadratic speedup. As the QRD algorithm is an application of the QPDE algorithm, it too inherits a quadratic quantum speedup.

In the Supplementary Information (SI) associated with this Paper we describe how Novak's Quantum Integration Algorithm (QIA) is constructed. This algorithm is seen to rely on the Quantum Amplitude Estimation Algorithm (QAEA) [19] to do its work. The SI then describes the construction of the QAEA which, in turn, uses the Quantum Phase Estimation Algorithm (QPEA) [20] to do its work. The latter algorithm is well-known and described in textbooks on quantum computing [21]. The QPDE algorithm is seen to rely on a Russian doll-like hierarchy of quantum algorithms that make use of three quantum oracles: one in Novak's QIA, and two in the QPEA. Ref. [22] presented quantum circuits that implement all three oracles and determined the quantum resources needed to implement them. The SI recaps the quantum resources discussion, as well as the issue of quantum speedup for quantum algorithms using quantum oracles that are implemented with quantum circuits.

## 4 Verification Problem

To verify the QRD algorithm we consider a radiation source at temperature $T_0$ in contact, through a planar interface, with a cold, semi-infinite, optically thick slab of matter. As discussed earlier, local thermodynamic equilibrium is assumed so that the radiation entering the slab at $x = 0$ evolves according to the NRDE. As the radiation diffuses, it heats the matter, giving rise to a travelling thermal front known as a Marshak wave [12]. The Marshak wave problem is a standard test problem for evaluating the quality of numerical solutions of the NRDE.

Following Marshak, we assumed the diffusion is one-dimensional, and that hydrodynamic effects can be ignored so that the matter remains at rest and at constant density $\rho_0$. We further assume that the Rosseland mean free path has a power-law dependence,

$$\lambda_R(\rho, T) = \lambda_0 \left(\frac{\rho}{\rho_0}\right)^{\nu} \left(\frac{T}{T_0}\right)^{\gamma}, \tag{4}$$

where $\lambda_0$ is a characteristic length-scale. Note that for our purposes, the density factor on the RHS disappears as $\rho$ is constant. The simulations discussed below used: $\gamma = 5.6$; boundary conditions $\varepsilon(0, t) = aT_0^4$ and $\varepsilon(\infty, t) = aT_i^4$ with $T_i \ll T_0$; and initial condition $\varepsilon(x, 0) = aT_i^4$ for $0 < x < \infty$.

To begin we rewrite the NRDE in dimensionless form. We define the characteristic energy density $\varepsilon_0 = aT_0^4$ and the dimensionless energy density $\overline{\varepsilon} = \varepsilon/\varepsilon_0$. We also define dimensionless time $\tau = ct/\lambda_0$ and position $z = x/\lambda_0$. With these definitions the NRDE becomes,

$$\frac{\partial \varepsilon}{\partial \tau} - \frac{\partial}{\partial z}\left[D(\varepsilon)\frac{\partial \varepsilon}{\partial z}\right] = 0, \tag{5}$$

where we have supressed the "bar" in $\overline{\varepsilon}$, and $D(\varepsilon) = \varepsilon^{\gamma/4}/3$. The boundary conditions are now $\varepsilon(0, \tau) = 1$ and $\varepsilon(\infty, \tau) = (T_i/T_0)^4$, and the initial condition is $\varepsilon(z, 0) = (T_i/T_0)^4$.

As seen earlier, the first step in applying the QRD algorithm to (5) is to discretize space. We thus introduce a spatial grid with $M$ grid-points $z_1, \ldots, z_M$. The second term on the RHS of (5) is approximated using a first-order forward difference approximation for the outer spatial derivative and a first-order backward difference for the inner spatial derivative. The result is the first-order accurate driver function $f_I(\varepsilon)$,

$$f_I(\varepsilon) = \frac{D_{I+1}\varepsilon_{I+1} - (D_{I+1} + D_I)\varepsilon_I + D_I\varepsilon_{I-1}}{\Delta z^2}, \tag{6}$$

where $\varepsilon_I(\tau) = \varepsilon(z_I, \tau)$, $D_I(\varepsilon) = (\varepsilon_I)^{\gamma/4}/3$, and $\Delta z$ is the spacing between grid-points. The spatial discretization reduces (5) to the system of ODEs appearing in (2) with (6) inserted on the RHS. The initial condition used in the simulations is $\varepsilon_I(0) = 0.01$ $(2 \le I \le M - 1)$, and the boundary conditions are $\varepsilon_1(\tau) = 1$ and $\varepsilon_M(\tau) = 0.01$.

The second step in the QRD algorithm is to use Kacewicz' quantum ODE algorithm to solve (2) with the given driver function $f_I(\varepsilon)$ and initial and boundary conditions. To that end, we numerically simulated determining an approximate solution of this ODE problem using Kacewicz' quantum algorithm. To test the quality of the quantum simulation results, we also used a standard PDE solver to obtain an approximate solution of (5) with the given initial and boundary conditions. We compared the resulting solution with that of the quantum simulation. These results appear in Fig. 1.

For the quantum simulation we used four different grid-sizes $M = 151, 201, 301, 401$, and a single grid-size $M = 401$ for the standard PDE solver. The standard PDE solver solution is plotted in all four subfigures so that convergence of the quantum solution to it can be seen as the grid-size $M$ increases. In each subfigure, the solid curves give the results of the standard PDE solver simulation, while the "crosses" are the results of the quantum simulation. Each subfigure shows the propagating Marshak wave at five different times. We see that, even for the smallest grid-size, $M = 151$, the agreement between the two simulations is quite good. The agreement increases as the grid-size increases, so that the two simulations are indistinguishable at $M = 401$. There is thus excellent agreement between the quantum and standard simulations.

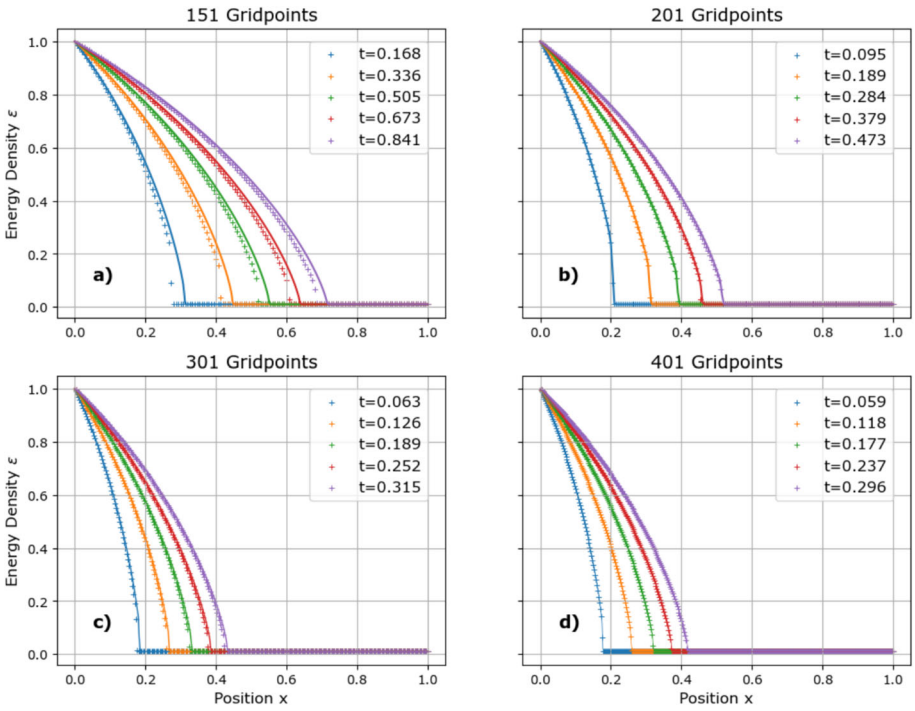


**Fig. 1** *Comparison of quantum and standard PDE solver simulation results for the Marshak wave problem.* We compare the approximate solution found through numerical simulation of the QRD algorithm applied to the Marshak wave problem with that found using a standard PDE solver. The quantum simulation was done using four different grid-sizes ($M = 151, 201, 301, 401$), while a single grid-size was used for the standard PDE solver ($M = 401$). Figures 1a-1d present the quantum simulation results for grid-sizes $M = 151, 201, 301, 401$, respectively, each at five different times. Each subfigure also plots the standard PDE solver result. The "crosses" are the quantum solution and the solid curves give the standard PDE solver solution. We see that agreement between the quantum and standard solutions is excellent, and indistinguishable for $M = 401$

## 5 Discussion

In this Paper we introduced a quantum algorithm that simulates the dynamics of nonlinear radiation diffusion with a quadratic quantum speedup. We verified the algorithm by applying it to a standard test problem of nonlinear radiation diffusion—a Marshak wave propagating through a cold, optically thick, semi-infinite slab of matter. We numerically simulated application of the QRD algorithm to this problem and compared the results with those produced by a standard PDE solver. Excellent agreement was found.

As noted in the Introduction, the design of an ICF experiment makes heavy use of computationally expensive radiation hydrodynamics codes which simulate radiation diffusion, hydrodynamic flows, and thermonuclear burn. The significance of the QRD algorithm is two-fold. First, it makes possible quantum simulation of radiation diffusion with a quadratic quantum speedup. Second, together with the quantum Navier-Stokes algorithm [10], quantum algorithms with quadratic speedups now exist that can carry out two of the three core tasks required to implement a quantum algorithm for radiation hydrodynamics. A major focus of future work is construction of a quantum algorithm that simulates the thermonuclear (TN)

burn of an ICF capsule with a quantum speedup. The overall structure of such an algorithm is clear. When TN burn is present, the matter energy-balance PDE must be decomposed into ion and electron contributions. The two resulting matter PDEs are coupled through terms arising from the Coulomb interaction. Note that fusion rate equations do not need to be solved to account for the fusion process. Instead, given the temperature and density, and assuming that the reacting ions are in a Maxwellian distribution, the fusion reactivity is tabulated, and a fusion energy source term is determined and added to the ion equation. The resulting system of PDEs, including radiation diffusion and hydrodynamics, is then solved using the QPDE algorithm.

Our ultimate goal is to apply the QPDE algorithm to the simulation of the spherically symmetric implosion of an ICF capsule. There exist many situations in the modeling of an ICF capsule where the matter is not optically thick. This can occur in carboy forms, low density materials, and high temperatures. In these situations, the matter and radiation temperatures may not be equal. The non-equilibrium Marshak wave problem [23] allows this important physical situation to be studied. Unlike the equilibrium Marshak wave problem considered here, in the non-equilibrium problem, matter and radiation are not assumed to be in local thermodynamic equilibrium with each other and so their local temperatures will not, in general, be equal. To account for this change, it is necessary to: (i) introduce the matter energy-balance PDE which must be simultaneously solved with the NRDE; and (ii) include terms in each that dynamically couple the radiation and matter. This allows for a much richer dynamics and the approach to mutual local thermodynamic equilibrium to be studied. Work to extend the QRD algorithm to treat this problem is currently underway.

Computational algorithms for solving PDEs fall into two broad categories: explicit and implicit. Each algorithm type has its pros and cons. Explicit algorithms are straightforward to implement, though auxiliary conditions are needed to insure computational stability. On the other hand, implicit algorithms are more complicated to implement, though usually yield more stable computations, and often can be proved to be unconditionally stable. Which is best to use depends upon the application, so a good computational toolbox should be able to implement both. For radiation hydrodynamics applications arising in the design of ICF experiments, it is important that implicit algorithms are available. Because of the disparate time scales associated with radiation diffusion and hydrodynamic flows, present-day radiation hydrodynamics codes simulate radiation diffusion implicitly, while hydrodynamic flows are simulated explicitly. Ref. [11] showed that the QPDE algorithm (and hence the QRD algorithm) is an explicit quantum algorithm. It also showed how the QPDE algorithm could be implemented as an implicit quantum algorithm. Work has begun to write simulation code for the implicit QRD algorithm, and to apply it to an appropriate verification problem.

**Supplementary Information** The online version contains supplementary material available at https://doi.org/10.1007/s10773-024-05800-x.

**Acknowledgements** We thank C. Yang for his help early in this project with the Marshak wave simulation software. F. Gaitan would like to thank T. Howell III for continued support. Part of this work was performed under the auspices of the U.S. Department of Energy by Lawrence Livermore National Laboratory under contract DE-AC52-07NA27344. Lawrence Livermore National Security, LLC.

**Author Contributions** F. Ga. co-wrote the manuscript, wrote the original simulation software that was adapted to the Marshak wave problem, and contributed to simulation data acquisition. F. Gr. co-wrote the manuscript and was lead on simulation data acquisition. M. P. contributed to Marshak wave simulation software.

**Data Availability** No datasets were generated or analysed during the current study.

## Declarations

**Competing Interests** F. Gaitan is a Quantum Information Processing Editorial Board Member.



## References

1. Chang, K.: Scientists Achieve Nuclear Fusion Breakthrough With Blast of 192 Lasers. New York Times (2022)
2. Zylstra, A.B., et al.: Experimental achievement and signatures of ignition at the National Ignition Facility. Phys. Rev. E **106**, 025202 (2022)
3. Abu-Shawareb, H., et al.: Lawson criterion for ignition exceeded in an inertial fusion experiment. Phys. Rev. Lett. **129**, 075001 (2022)
4. Hurricane, O.A., et al.: Fuel gain exceeding unity in an inertially confined fusion implosion. Nature **506**, 343–348 (2020)
5. Marinak, M.M., Kerbel, G.D., Gentile, N.A., Jones, O., Munro, D., Pollaine, S., Dittrich, T.R., Haan, S.W.: Three-dimensional HYDRA simulations of National Ignition Facility targets. Phys. Plasmas **8**, 2275–2280 (2001)
6. Marinak, M.M., Haan, S.W., Dittrich, T.R., Tipton, R.E., Zimmerman, G.B.: A comparison of three-dimensional multimode hydrodynamic instability growth on various National Ignition Facility capsule designs with HYDRA simulations. Phys. Plasmas **5**, 1125–1132 (1998)
7. Fryxell, B., et al.: FLASH: an adaptive mesh hydrodynamics code for modeling astrophysical thermonuclear flashes. Astrophys. J. Suppl. Ser. **131**, 273–334 (2000)
8. Dubey, A., et al.: Extensible component-based architecture for FLASH, a massively parallel, multiphysics simulation code. Parallel Comput. **35**, 512–522 (2009)
9. Tzeferacos, P., et al.: FLASH MHD simulations of experiments that study shock-generated magnetic fields. High Energ. Dens. Phys. **17**, 24–31 (2015)
10. Gaitan, F.: Finding flows of a Navier-Stokes fluid through quantum computing. npj Quantum Inform. **6**, 61 (2020)
11. Gaitan, F.: Finding solutions of the Navier-Stokes equations through quantum computing - recent progress, a generalization, and next steps forward. Adv. Quantum Tech. **4**, 2100055 (2021)
12. Marshak, R.E.: Effect of radiation on shock behavior. Phys. Fluids **1**, 24–29 (1958)
13. Zel'dovich, Y.B., Raizer, Y.P.: Physics of shock waves and high-temperature hydrodynamic phenomena. Dover, New York (2002)
14. Graziani, F.: Radiation diffusion: an overview of physical and numerical concepts. United States N. p. 2005. https://doi.org/10.1142/9789812703446_0002
15. Kacewicz, B.: Almost optimal solution of initial-value problems by randomized and quantum algorithms. J. Complex. **22**, 676–690 (2006)
16. Gautschi, W.: Numerical analysis. Birkäuser, New York (2012)
17. Iserles: A first course in the numerical analysis of differential equations (Cambridge, New York) (2009)
18. Novak, E.: Quantum complexity of integration. J. Complex. **17**, 2–16 (2001)
19. Brassard, G., Hoyer, P., Mosca, M., Tapp, A.: Quantum amplitude amplification and estimation, preprint, http://arXiv.org/quant-ph/0005055 (2000)
20. Kitaev, A.: Quantum measurements and the Abelian Stabilizer Problem, preprint, http://arXiv.org/quant-ph/9511026 (1995)

21. Nielsen, M.A., Chuang, I.L.: Quantum Computation and Quantum Information (Cambridge, New York) (2000)
22. Gaitan, F.: Circuit implementation of oracles used in a quantum algorithm for solving nonlinear partial differential equations. Phys. Rev. A **109**, 032604 (2024)
23. Pomraning, G.C.: The non-equilibrium Marshak wave problem. J. Quant. Spectrosc. Radiat. Transfer **21**, 249–261 (1979)
24. Courant, R., Friedrichs, K.O., Lewy, H.: Über die partiellen differenzengleichungen der mathematischen physik. Math. Ann. **100**, 32–74 (1928). (Translation: On the partial difference equations of mathematical physics. IBM J. Res. Dev. **11**, 215-234 (1967).)